Proceedings of the ASME 2018 37th International Conference on Ocean, Offshore and Arctic Engineering
OMAE2018
June 17-22, 2018, Madrid, Spain

OMAE2018-78376

DIRECT SIMULATIONS OF TURNING CIRCLE MANEUVER IN WAVES USING RANS-OVERSET METHOD

Jianhua Wang
Collaborative Innovation Center for Advanced Ship and Deep-Sea Exploration
State Key Laboratory of Ocean Engineering
School of Naval Architecture, Ocean and Civil Engineering
Shanghai Jiao Tong University
Shanghai, 200240, China

Decheng Wan*
Collaborative Innovation Center for Advanced Ship and Deep-Sea Exploration
State Key Laboratory of Ocean Engineering
School of Naval Architecture, Ocean and Civil Engineering
Shanghai Jiao Tong University
Shanghai, 200240, China
*Corresponding author: dcwan@sjtu.edu.cn

ABSTRACT

In the present work, a RANS-overset method is used to numerically investigate turning circle maneuver in waves for a twin-screw ship. CFD solver naoe-FOAM-SJTU is used for the numerical computations of the fully appended ONR Tumblehome ship model. Overset grids are used to fully discretize the ship hull, twin propellers and rudders. The simulation of turning circle maneuver is carried out at constant propeller rotational speed with 35° rudder deflection. Open source toolbox waves2Foam is utilized to generate desired waves for the moving computational domain. Predicted ship trajectory and 6DoF motions, hydrodynamic forces and moments acting on the ship and the moving components are presented. The main parameters of the turning circle maneuver, such as the advance, the transfer, the tactical diameter, and the turning diameter, are presented and compared with the available experiment. Wave effects on the free running turning circle maneuver are discussed through detailed flow visualizations. The trajectory and main parameters agree well with the experiment, which show that the present RANS-overset method is a reliable approach to directly simulate turning circle maneuver in waves.

INTRODUCTION

Turning ability is very important for the navigation of a naval ship and it can be estimated by turning circle test. Generally, turning circle maneuver is achieved by the steering operation with the rudder. As a result, it is of great importance to consider the movement of rudders during the simulation in order to reappear the realistic operational scenario. Most early researches focused on the turning circle maneuver were using ship model test in a maneuvering basin. Sanada et al.[1] conducted turning circle test using the free running ship model in IIHR wave basin and the tests were also conducted for various wave conditions with different headings and wave parameters. Though the experiment test can be a reliable way to predict the turning ability of a ship, the expense to conduct such complex tests is still very high. Numerical approaches have long been proposed to predict the turning ability. Previous studies regarding the numerical method were mostly using the system-based (SB) method, where prescribed mathematical model and maneuvering coefficients were required. Yasukawa and Yoshimura[2] used the Maneuvering Modeling Group (MMG) model to conduct maneuvering simulations for KVLCC2 tanker in both model and full scale. Rajesh and Bhattacharyya[3] applied nonparametric system identification to a nonlinear maneuvering model for large tankers using artificial network method. Obvious deviations were found in the above studies for the maneuvering motion compared with the model tests.

Apart from the free running model tests and the system based method, computational fluid dynamics (CFD) has become a reliable tool to predict ship maneuvering performance. Carrica et al.[4] conducted URANS simulations for turn and zigzag maneuvers of a surface combatant using dynamic overset grids. Broglia et al.[5] and Dubbioso et al.[6] studied the turning ability for a fully appended twin screw vessel considering single and twin rudder configuration, respectively. In their studies, overset grids were used to discretize the rudder while the propellers were using the

simplified actuator disk model. Consequently, the predicted results showed reasonable errors with the free running ship tests. Shen et al.[7] implemented overset grid into OpenFOAM and applied the technique to simulate zigzag maneuver. Wang et al.[8] further extended the solver in calculating turning circle maneuver with fully discretized propellers and rudders. All the above researches proved that the overset grid method was a robust and reliable approach to numerically predict ship maneuvering performance.

However, Previous CFD simulations for free running ship maneuver were mostly done for the calm water conditions. CFD techniques should be improved to extend its ability to investigate ship maneuvering in waves since it is closest to the practical situation. In the present work, dynamic overset grid method is adopted to handle with the complex motion of ship hull-propeller-rudder system, while the open source wave generation tool waves2Foam[9] is utilized to generate desired waves in moving computational domain. Through this way, direct RANS computations for turning circle maneuver in waves are carried out.

NUMERICAL APPROACH

Numerical computations are using the ship hydrodynamics CFD solver, naoe-FOAM-SJTU[10,11], developed on the open source platform OpenFOAM. The solver has been extensively validated on large amount of ship hydrodynamic cases, e.g. ship resistance[12,13], seakeeping[14–16], propulsion[7,17,18] and maneuvering[8,19]. Only main features are introduced herein, more detailed information can be found in the references mentioned above. The solver has the dynamic overset grid capability and includes a full 6DoF motion module with a hierarchy of bodies, making it easy to directly simulate ship maneuver with rotating propellers and moving rudders. In general, naoe-FOAM-SJTU solves the Reynolds-averaged Navier-Stokes (RANS) equations for unsteady turbulent flows around complex geometries. Volume of fluid (VOF) approach with bounded compression technique[20] is used to capture free surface around ship hull. The blended $k-\varepsilon$, $k-\omega$ shear stress transport (SST) turbulence model[21] is employed to model the turbulence features. Wall functions are used to model the velocity gradient effects near the wall.

The computational domain is discretized by multi unstructured overlapping grids, and the space discretization is using the finite volume method (FVM). Besides, the pressure-implicit split-operator (PISO) algorithm[22] is applied for solving the pressure-velocity coupling equations. In addition, several built-in discretization schemes in OpenFOAM are used to solve the partial differential equations (PDE): the implicit Euler scheme is used for temporal discretization; second order total variation diminishing (TVD) scheme is used to discretize the convection term in momentum equation; a central differencing scheme is applied for diffusion terms.

As mentioned in the introduction part, the open source wave generation tool waves2Foam is utilized to generate desired wave environment. The toolbox adopts a relaxation technique for wave generation and absorption and has obvious advantage over traditional numerical wave tank with velocity-inlet boundary. Figure 1 illustrates the wave generation zone in the present computations, where a circular ring form zone is used to generate waves. During the simulations, the zone is frozen to the computational domain and the waves can therefore propagate to the near ship region regarding the turning circle maneuver.

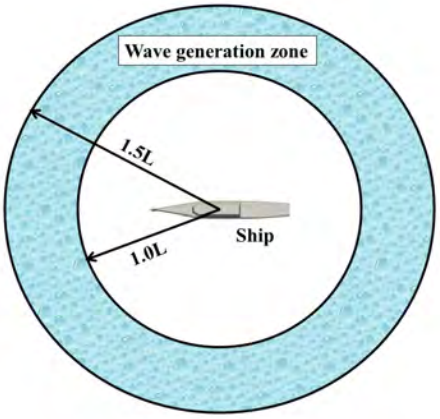

Figure 1 Diagram of wave generation zone

GEOMETRY AND GRIDS

In the present work, the ONR Tumblehome ship model 5613, which is a preliminary design of a modern surface combatant fully appended with skeg and bilge keels, is used for the numerical simulations. The ship model also has rudders, shafts and propellers with propeller shaft brackets. The geometry of ONR Tumblehome is shown in Figure 2, and the main particulars are listed in Table 1. The ship model is used as the benchmark case of free running ship in Tokyo 2015 CFD workshop in ship hydrodynamics. Extensive experiments were performed at IIHR basin for this ship model and the available experimental data can be used to validate our computational results.

Figure 2 Geometry model of ONRT

Table 1 Principle particulars of ONRT model

Parameters	Variable	Value	Unit
Length	L_{WL}	3.147	m
Width	B_{WL}	0.384	m
Draft	T	0.112	m

Displacement	Δ	72.6	kg
Longitudinal center	LCB	1.625	m
Vertical center	KG	0.156	m
Moment of inertia	K_{xx} / B_{WL}	0.444	
Moment of inertia	$K_{yy}, K_{zz} / L_{WL}$	0.246	
Propeller diameter	D_P	0.1066	m
Shaft angle	ε	5	deg.
Max rudder rate	r_R	35	deg./s

In order to directly simulate the free running ship maneuver in waves, six part of overlapping grids are used to discretize the computational domain: one for the background grid, one for the grid around the ship hull, two for the grids around the two propellers on starboard side and port side respectively, two parts for the twin rudders. The detailed overset grid arrangements are shown in Figure 3. Unstructured grids are generated by the pre-processing utilities provided by OpenFOAM. Local grid distribution around ship hull, propeller and rudder is shown in Figure 4. It should be noticed that artificial gaps between propeller and shaft, rudder and rudder root are used to obtain enough interpolation cells. Near-wall grid spacing is designed to meet the requirement of turbulence model using wall functions. The total grid number for the free-running simulations is 7.13 million. The motion of grid around propeller and rudder follow the control laws of specific ship maneuver.

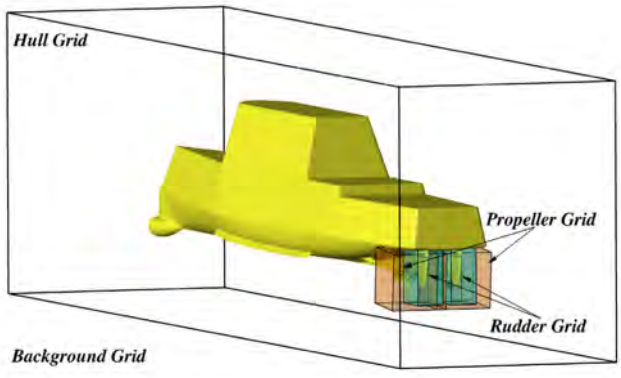

Figure 3 Overset grid arrangement

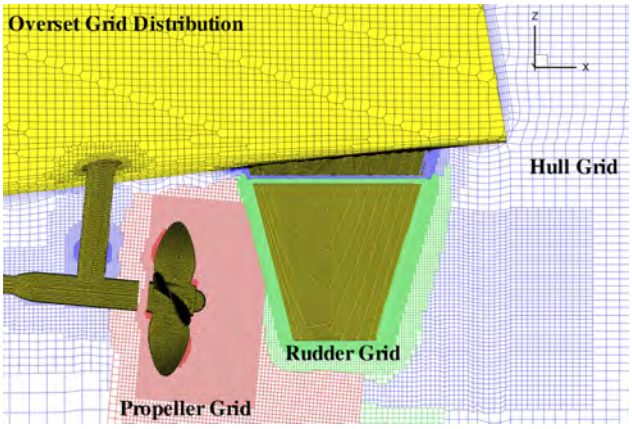

Figure 4 Overset grid distribution

NUMERICAL SIMULATIONS

The present simulation case is the standard turning circle maneuver with 35° rudder deflection turning to starboard. The initial ship speed is U=1.11m/s with corresponding Froude number of 0.20. During the simulation, the rotational speed of propellers is set fixed with constant value (8.819 RPS, underestimated by 1.7% compared with the experiment) according to the previous CFD simulation of self-propulsion in calm water[19]. The rudder is controlled regarding to the standard turning circle maneuver. The incident wave parameters follow the experimental setup[1,23], where the wave length equals ship length (λ=L_{WL}) and wave steepness (H / λ) is 0.02. The initial flow state of the turning circle maneuver computation is from the stable state of self-propulsion condition, then the ship model is released in 6 degrees of freedom with specified rudder control to achieve the turning circle maneuver motion.

Numerical calculations are carried out on the HPC cluster center in Computational Marine Hydrodynamics Lab (CMHL), Shanghai Jiao Tong University. Each node consists of 2 CPUs with 20 cores per node and 64GB accessible memory (Intel Xeon E5-2680v2 @2.8 GHz). 40 processors are assigned to calculate the turning circle maneuver in waves, in which 38 processors are for the flow calculation and the other 2 processors are used for interpolation calculation of overset grids. The time step was set to $\Delta t = 0.0005s$, which corresponds to approximately 1.5 degrees of propeller rotation per time step. It costs approximately 1206 hours of clock time with about 155000 time steps to complete the computation in in waves.

Figure 5 shows the predicted trajectory for turning circle maneuver compared with the experimental measurements. The CFD results of circle trajectory is larger than that of experiment. It is mainly due to the modification of rudder geometry, which is slightly smaller in the computation to get enough interpolation cells. Consequently, the effective rudder area is smaller, which leads to the insufficient turning ability. Through the comparison we can see that there are obvious

oscillations for the trajectory with the heading angle change around 90° and 270°. Local curves are enlarged in Figure 6 to better show the fluctuation. Despite the deviation from the experimental data, the wave effects on the trajectory can be captured well using the present approach.

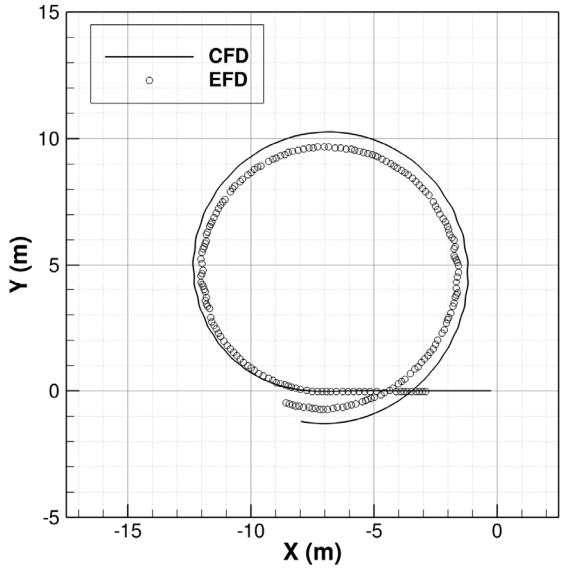

Figure 5 Trajectory comparison of turning circle maneuver in waves

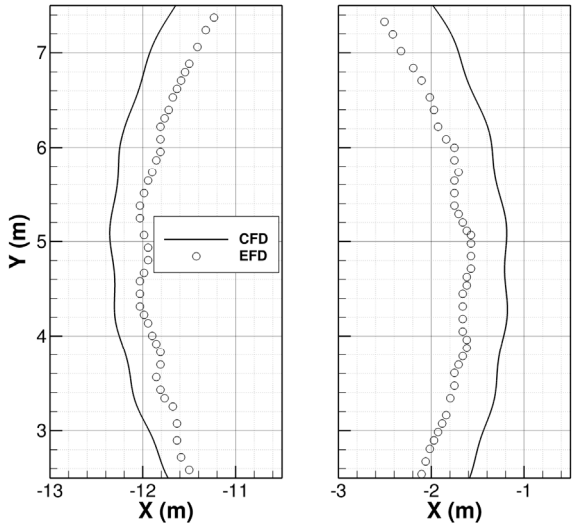

Figure 6 Local view of trajectory for heading angle around 90° and 270°

It can be seen that the predicted oscillations of the trajectory is weaker than that of the experiment measurement, which indicates that the turning ability for the CFD model is not as good as the actual ship model in the experiment. This also explains the larger range of the trajectory predicted by CFD computation.

The comparisons of the main parameters of turning circle maneuver, i.e. advance, transfer, tactical diameter, turning diameter as well as time to 90°/180° heading change, are shown in Table 2. The time is shifted to the same rudder execution time so as to give the correct comparison of when to achieve 90° or 180° heading change. The predicted results show good agreement with the experiment measurement performed at IIHR wave basin[23,24], where the error is within 10%. Present numerical approach can give an overall evaluation of the maneuvering behavior in waves.

Table 2 Comparisons of turning circle parameters

Parameters		CFD	EFD[23]	Error
Advance (m)	A_D	6.9171	6.9978	-1.15%
Transfer (m)	T_R	4.1063	3.8797	5.84%
T_{90} (s)		12.2822	11.5700	6.15%
Tactical (m)	T_A	10.1838	9.6213	5.85%
T_{180} (s)		24.5894	22.4100	9.72%
Turning (m)	T_D	10.2807	9.6464	6.57%

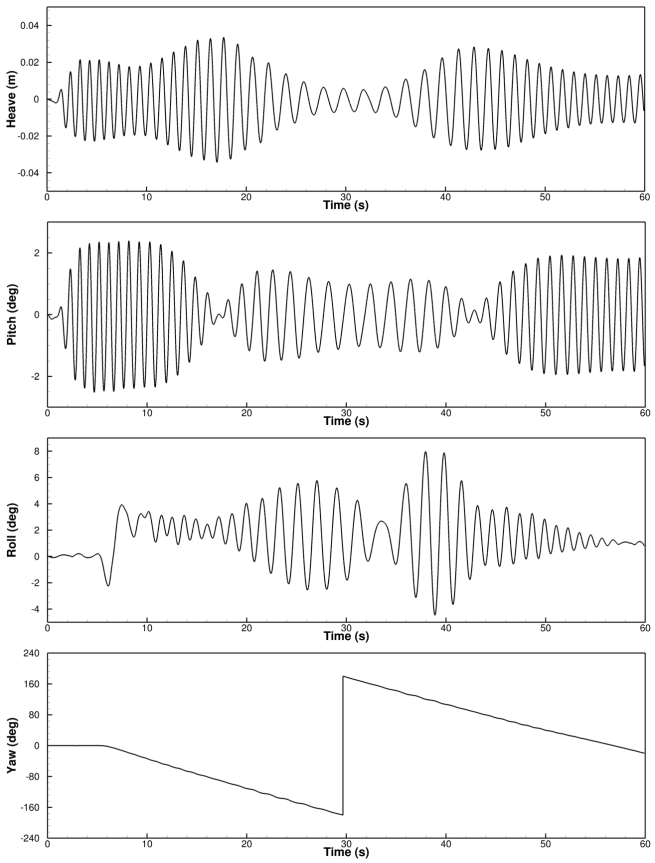

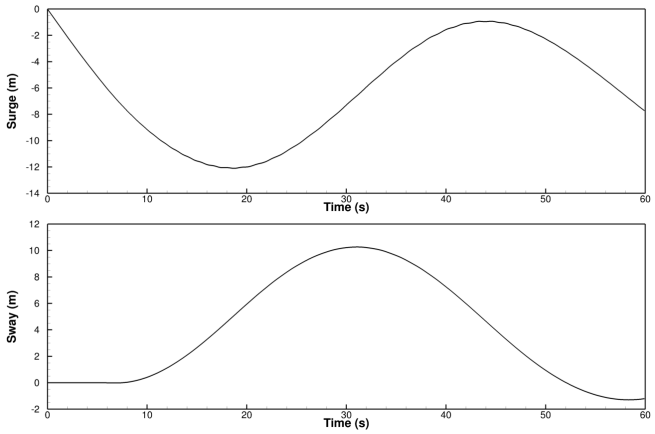

Figure 7 Time histories of ship motions: a) heave, b) pitch, c) roll, d) yaw, e) surge, f) sway

Figure 7 presents the time histories of ship 6DoF motions, i.e. heave, pitch, roll, yaw, surge and sway motion. The heave, pitch and roll motions experience significant wave induced motions. Despite the obvious wave induced motions, low frequency motion due to maneuvering motion can also be noticed. Maximum pitch angle during the turning circle motion is around 2.5° and the roll motion varies from -4.4° to 8°. The wave induced roll motion can be as large as the roll motion due to steering operation. However, the planar motions, namely yaw, surge and sway motion, experience less fluctuation behavior. In order to give better description of the motion performance during the turning circle maneuver, the ship motion in polar coordinate system are presented, where the radial coordinate stands for the motion amplitude and the angular coordinate represents the heading angle.

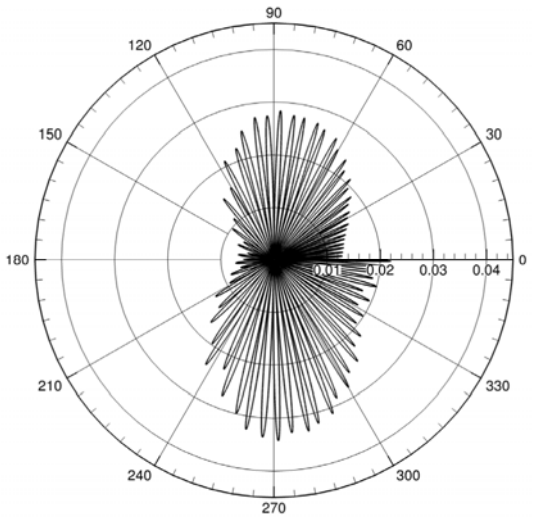

Figure 8 Magnitude of heave motion within one turn in polar coordinate system

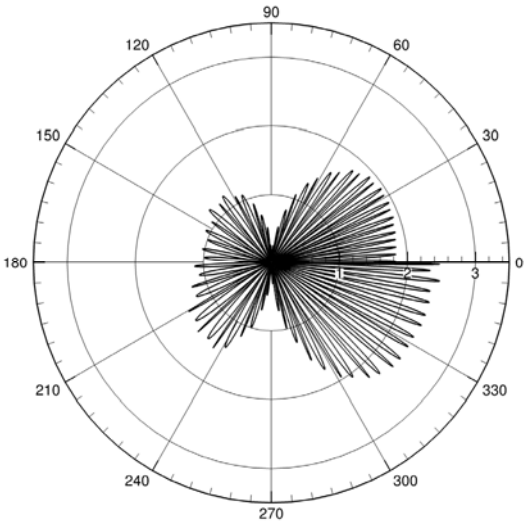

Figure 9 Magnitude of pitch motion within one turn in polar coordinate system

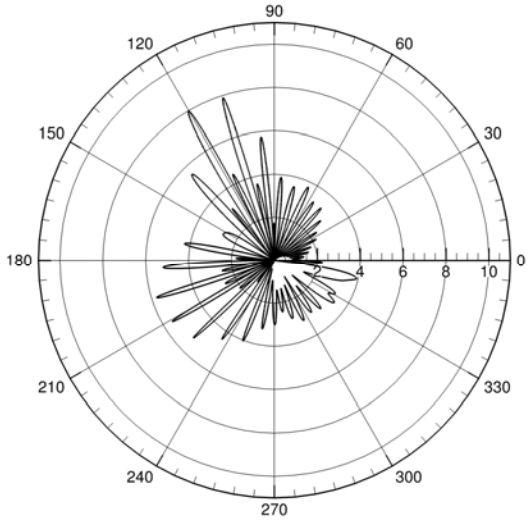

Figure 10 Magnitude of roll motion within one turn in polar coordinate system

As discussed before, the wave effects are more noticeable for heave, pitch and roll motion and only these three motions are presented to show the influences of waves associate with the heading angle. Figure 8 illustrates the magnitude of heave motion in one turn and it can be obviously seen that the heave motion is significantly enlarged when the ship experience beam sea condition. The pitch motion show the opposite behavior, where the pitch motion is remarkably increased when the ship is encountering head and following sea conditions. The ship roll motion is larger in following sea and it meets the peak value of 8° when the heading change is 120°. All the three figures illustrate the motion performance during the turning circle maneuvering in waves within one turn.

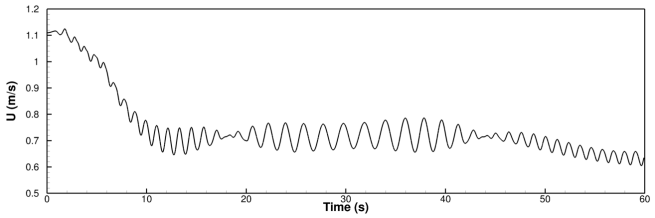

Figure 11 Time history of instantaneous ship speed

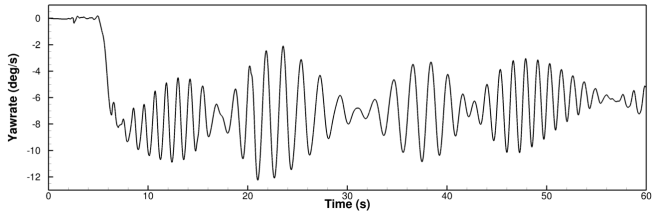

Figure 12 Time history of yaw rate

Figure 11 and Figure 12 show the time histories of instantaneous ship speed and yaw rate during the simulation time. It is clear that the ship speed loss is significant during the turning circle maneuver, where the speed loss can be as large as 40%. The ship speed first drops due to the incident waves and the rudder deflection, then the ship speed keeps a relatively average loss of 30% at the steady turning circle stage. For the yaw rate variation, it first increases due to the steering operation, then oscillates due to the change of the encountering waves. The maximum yaw rate can be 12.2 deg./s.

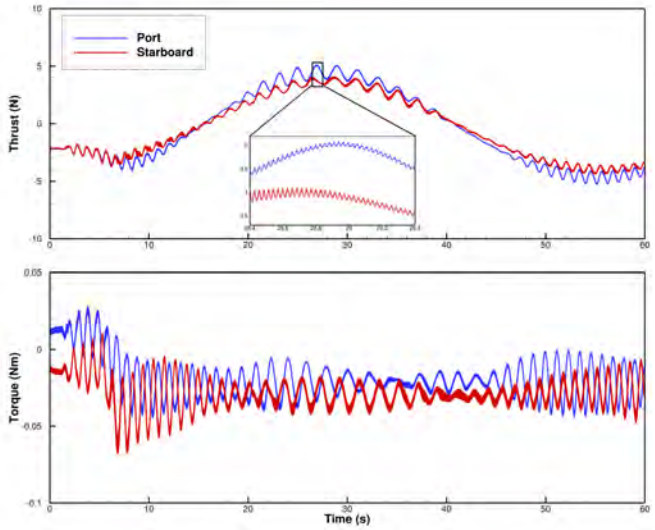

Figure 13 Time histories of thrust and torque

Figure 13 shows the time histories of thrust and torque during the turning circle maneuver in waves. At the beginning, the ship is advancing straight forward and the thrust variation for the port and starboard side are almost the same, while the torque variations are symmetric. As soon as the rudder executes, both thrust and torque become asymmetry. The curves show alternating amplitude of the fluctuations for the windward and leeward side propulsion forces. It can also be noticed of the very high frequency fluctuations due to the rotating propellers pass through the flow field from the enlarge view. Figure 14 presents the time variations of the hydrodynamic loads acting on the twin rudders during the turning circle maneuver in waves. The trends of variation are similar with the propulsion performance. The rudder resistance and lateral force are increasing remarkably due to the steering operation and the resultant lateral force lead to the turning behavior.

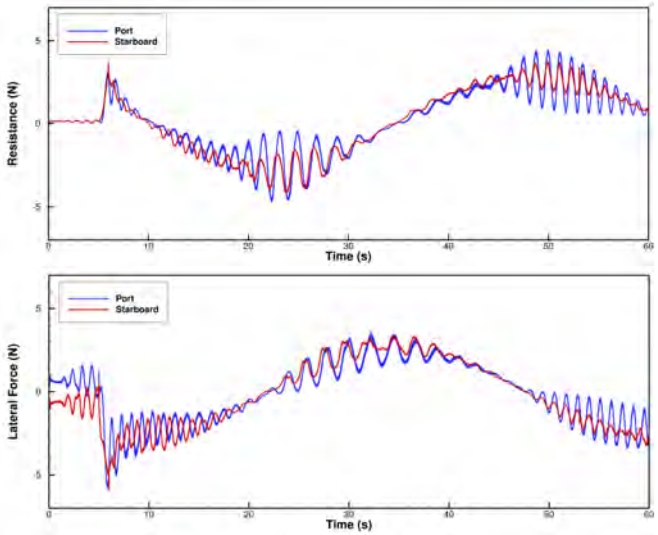

Figure 14 Time histories of hydrodynamic loads on twin rudders

In order to better understand the hydrodynamic loads of the twin rudders during the steering operation, here we give the transient force change shown in Figure 15. The two black lines mark the beginning and end of the steering operation. The resistance is the same and lateral force is symmetric before the rudder execution, while both of them increase obviously to a high level. The lateral forces of starboard and port side rudder reach 5 to 6N at the end of rudder execution.

Figure 16 illustrates the vortices around twin propellers and rudders during the rudder execution. Four snapshots with rudder angle equal 0°, 11.7°, 23.3° and 35° are presented to show the disturbance due to the rudder deflection. At time instance θ=0°, the vortices separated from propellers and rudders are almost symmetric, which explains the hydrodynamic performance at initial stage shown in Figure 14 and Figure 15. With the increase of the rudder angle, the aligned rudder starts to interfere with the propeller vortices. When the rudder turns to port side, the hub vortices of the port side propeller meets the aligned rudder, which result in the strong interaction between rudder vortices and hub vortices. As for the starboard side flow, the main interaction locates on the

propeller tip vortices and the rudder vortices. This different performance of starboard and port side rudder explains the discrepancy of hydrodynamic loads acting on both side rudders as well as propellers. The trajectory of propeller and rudder vortices also indicate that the ship is turning to starboard. Large flow separations are shown in the wake region around twin propellers and rudders, which can not be captured accurately using the present RANS approach. This is also one of the reasons that lead to the discrepancies between the CFD prediction and experiment results. More accurate turbulence model, such as DES or LES, needs to be applied to improve the present simulation accuracy.

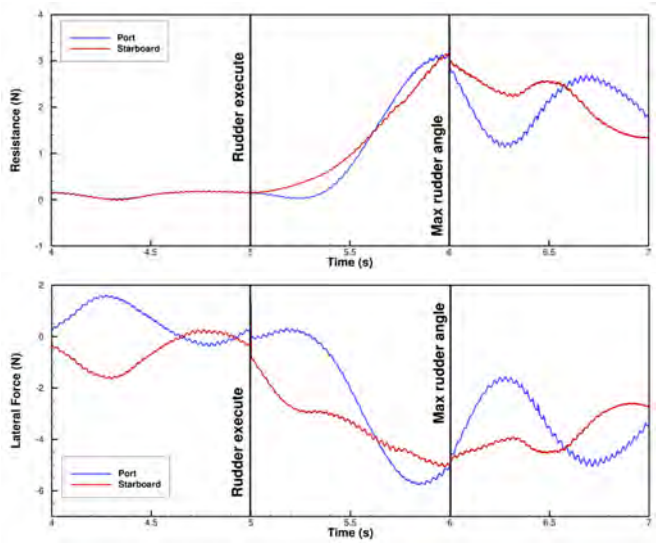

Figure 15 Rudder forces during rudder execution

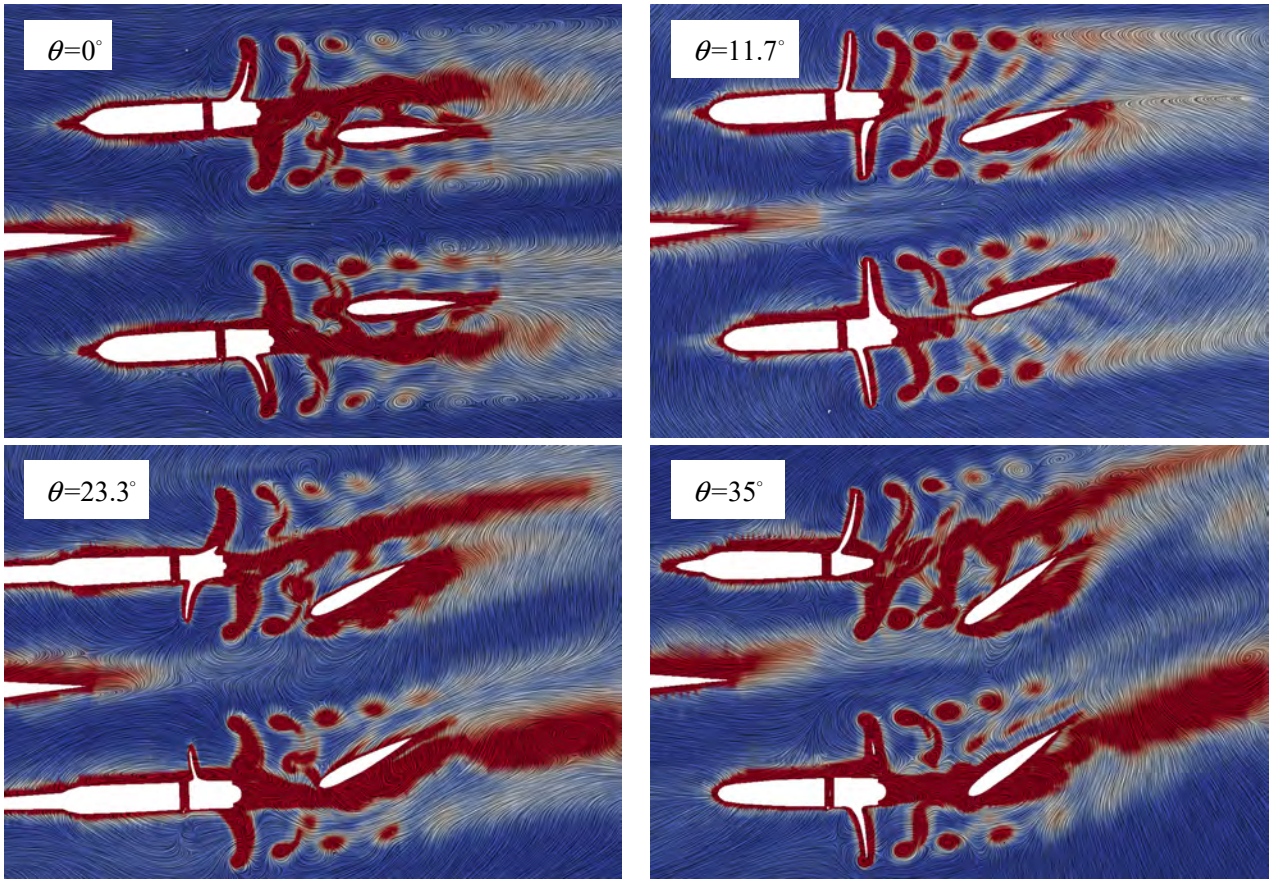

Figure 16 Vortical field around twin propellers and rudders during the steering operation

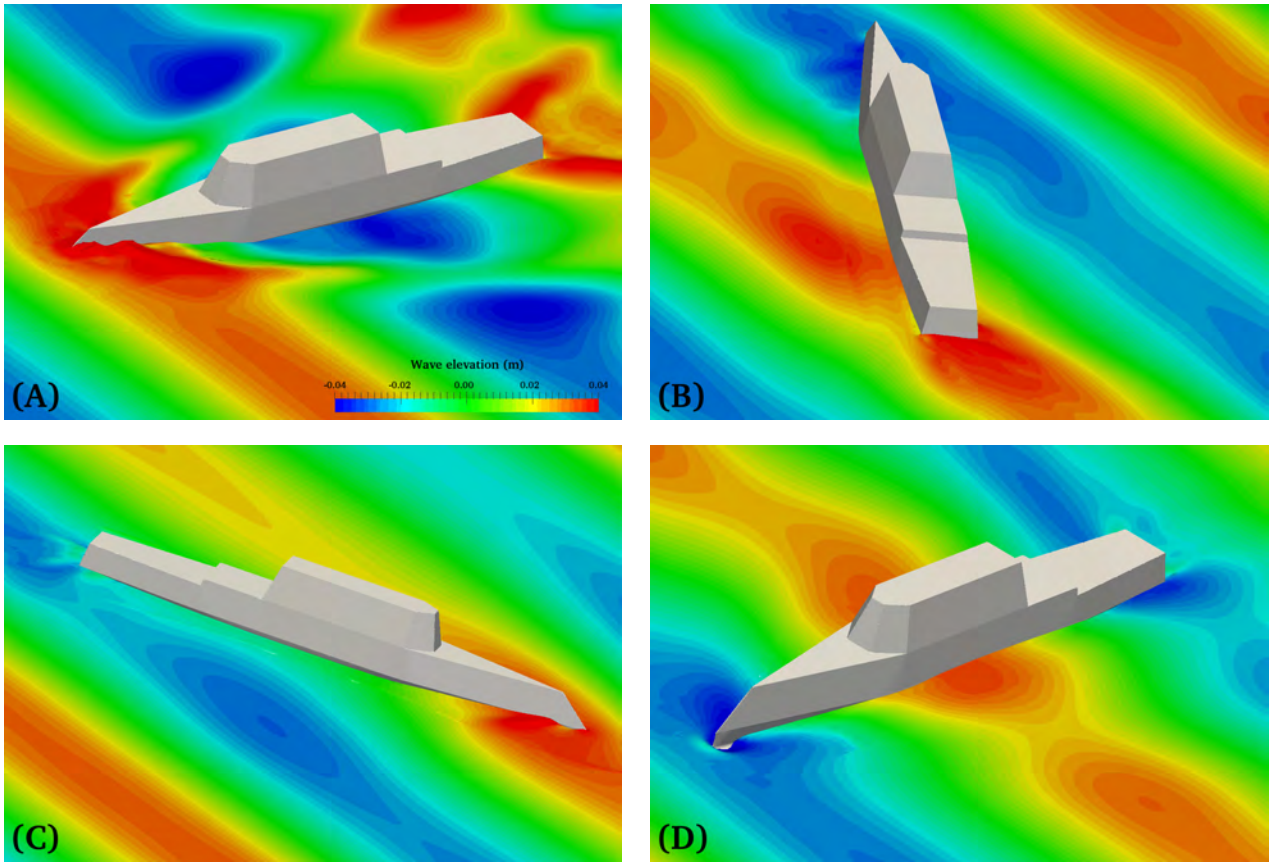

Figure 17 Free surface elevation during turning circle maneuver in waves (A: heading angle 0°, B: heading angle 120°, C: heading angle 240°, B: heading angle 360°)

Figure 17 illustrates four snapshots of free surface elevation during one period of turning circle maneuver, corresponding to heading angle of 0°, 120°, 240° and 360°. Free surface is colored by wave height. It can be noticed that at time instance A, the wave pattern is symmetric with the fact of the ship is just advancing straight forward. However, when the ship is under turning circle condition, the wave distribution is strongly different. As can be seen in time instances B, C and D, the bow wave and stern wave show much asymmetric, which will cause the pressure difference on both side of ship hull. From time instance D we can also observe that the ship bow is out of water when the bow encountering trough. It indicates that the ship motions are very large in the present wave condition during the turning circle maneuver.

3D vortical structure around ship hull, twin propellers and rudders are depicted in Figure 18 with the same time in Figure 17. The tip vortices and hub vortices of twin propellers can be resolved using the present approach. At time instance A, the vortices separated from propellers are barely disturbed by the aligned rudders, while strong interaction between the propellers and rudders can be noticed at the subsequent instances. For the port side flow, propeller hub vortices are cut off by the aligned rudder and rudder tip vortices are mixed with the tip vortices of propeller. Different from the port side behavior, there are two strong separate vortices in the starboard side. One is the hub vortices of propeller and another one is the tip vortices of rudder due to the large attack angle. This phenomena can also result in the highly difference of hydrodynamic loads acting on twin propellers and rudders.

CONCLUSIONS

In this paper, dynamic overset grid technique is applied to handle with complex ship motions with hull-propeller-rudder system. A circular ring form zone is used to generate waves during the simulation of turning circle maneuver. With the help of maneuvering control module and wave generation tool, direct computations of free running ship turning circle maneuver in waves is carried out using CFD solver naoe-FOAM-SJTU.

The main parameters of turning circle maneuver is presented and compared with the available experiment measurement. Good agreement is achieved with errors less than 10%. Predicted ship trajectory are also compared with the experiment results and both approaches can capture the

fluctuations when the ship is experiencing beam sea conditions. Heave, pitch and roll motions show strong relations with encountering waves, while the planar motions are less dependent on the waves. Particularly, the ship is experiencing large speed loss up to 40%. Propulsion performance and hydrodynamic loads acting on twin rudders are presented to illustrate the hydrodynamic behavior during the turning circle maneuver in waves. Discrepancies between port and starboard side forces are analyzed with detailed flow visualizations. Free surface elevations and vortical structures at four typical time instances are presented to show the wave influences and the interaction between the moving appendages.

Although the present CFD solver is proved reliable in predicting the maneuvering performance in waves, the computation cost is still very high. Future work will be focused on the improvement of the efficiency.

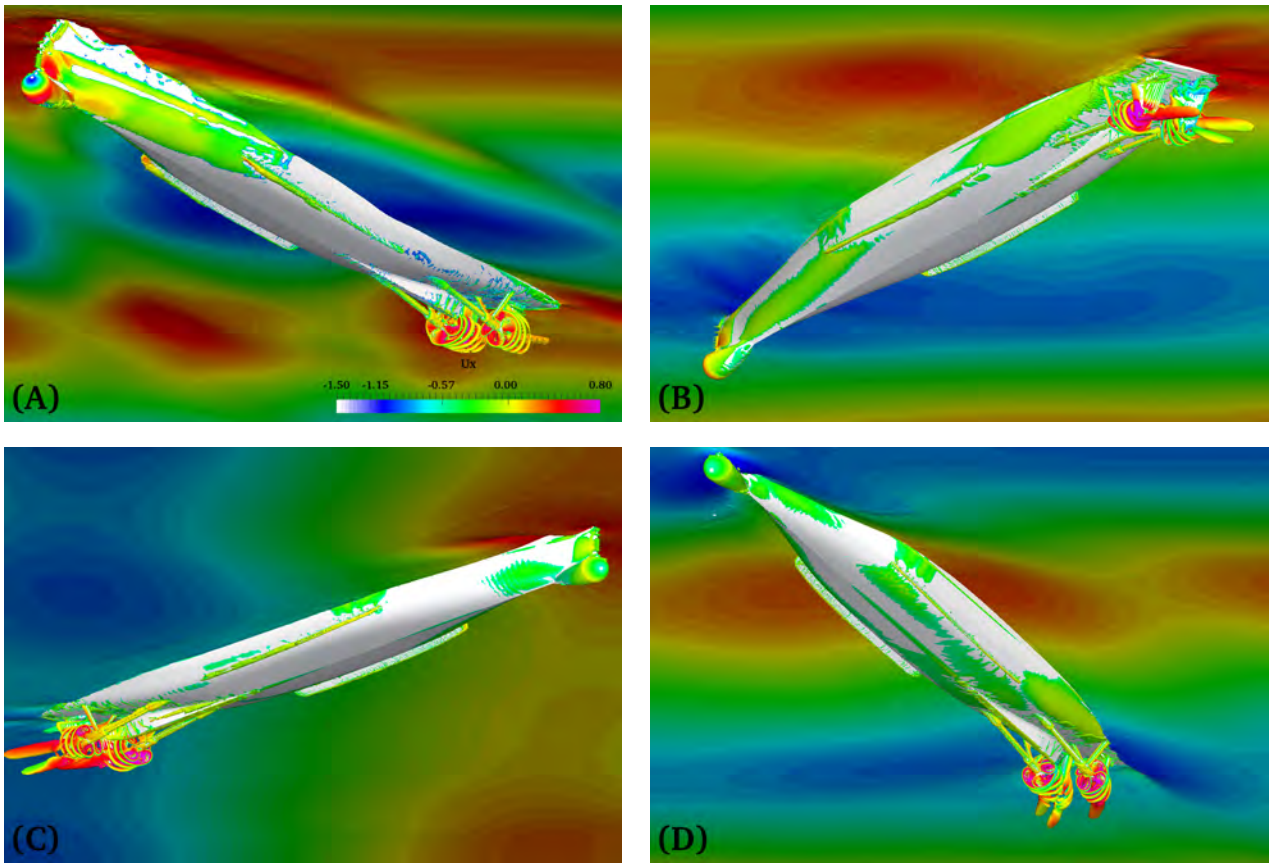

Figure 18 3D vortical structures around ship hull, twin propellers and rudders during turning circle maneuver in waves (A: heading angle 0°, B: heading angle 120°, C: heading angle 240°, B: heading angle 360°)

ACKNOWLEDGMENTS

This work is supported by the National Natural Science Foundation of China (51490675, 11432009, 51579145), Chang Jiang Scholars Program (T2014099), Shanghai Excellent Academic Leaders Program (17XD1402300), Program for Professor of Special Appointment (Eastern Scholar) at Shanghai Institutions of Higher Learning (2013022), Innovative Special Project of Numerical Tank of Ministry of Industry and Information Technology of China (2016-23/09) and Lloyd's Register Foundation for doctoral student, to which the authors are most grateful.

REFERENCES

[1] Sanada, Y., Tanimoto, K., Takagi, K., Gui, L., Toda, Y., and Stern, F. 2013, "Trajectories for ONR Tumblehome Maneuvering in Calm Water and Waves," Ocean Eng., **72**, pp. 45–65.

[2] Yasukawa, H., and Yoshimura, Y. 2015, "Introduction of MMG Standard Method for Ship Maneuvering Predictions," J. Mar. Sci. Technol., **20**(1), pp. 37–52.

[3] Rajesh, G., and Bhattacharyya, S. K. 2008, "System Identification for Nonlinear Maneuvering of Large Tankers Using Artificial Neural Network," Appl. Ocean Res., **30**(4), pp. 256–263.
[4] Carrica, P. M., Ismail, F., Hyman, M., Bhushan, S., and Stern, F. 2012, "Turn and Zigzag Maneuvers of a Surface Combatant Using a URANS Approach with Dynamic Overset Grids," J. Mar. Sci. Technol., **18**(2), pp. 166–181.
[5] Broglia, R., Dubbioso, G., Durante, D., and Di Mascio, A. 2015, "Turning Ability Analysis of a Fully Appended Twin Screw Vessel by CFD. Part I: Single Rudder Configuration," Ocean Eng., **105**, pp. 275–286.
[6] Dubbioso, G., Durante, D. Di Mascio, A., and Broglia, R. 2016, "Turning Ability Analysis of a Fully Appended Twin Screw Vessel by CFD. Part II: Single vs. Twin Rudder Configuration," Ocean Eng., **117**, pp. 259–271.
[7] Shen, Z., Wan, D.C. and Carrica, P. M. 2015, "Dynamic Overset Grids in OpenFOAM with Application to KCS Self-Propulsion and Maneuvering," Ocean Eng., **108**, pp. 287–306.
[8] Wang, J., Zhao, W., and Wan, D.C. 2016, "Free Maneuvering Simulation of ONR Tumblehome Using Overset Grid Method in naoe-FOAM-SJTU Solver," *Proceedings of 31th Symposium on Naval Hydrodynamics*, Monterey, USA.
[9] Jacobsen, N. G., Fuhrman, D. R., and Fredsøe, J., 2012, "A Wave Generation Toolbox for the Open-Source CFD Library: OpenFoam®," Int. J. Numer. Methods Fluids, **70**(9), pp. 1073–1088.
[10] Shen, Z., Cao, H., Ye, H., and Wan, D.C. 2012, *The Manual of CFD Solver for Ship and Ocean Engineering Flows: naoe-FOAM-SJTU*, Shanghai Jiao Tong University.
[11] Shen, Z., Zhao, W., Wang, J., and Wan, D.C. 2014, *Manual of CFD Solver for Ship and Ocean Engineering Flows: naoe-FOAM-SJTU*, Shanghai Jiao Tong University.
[12] Zha, R., Ye, H., Shen, Z., and Wan, D.C. 2015, "Numerical Computations of Resistance of High Speed Catamaran in Calm Water," J. Hydrodyn. Ser B, **26**(6), pp. 930–938.
[13] Zha, R., Ye, H., Shen, Z., and Wan, D.C. 2014, "Numerical Study of Viscous Wave-Making Resistance of Ship Navigation in Still Water," J. Mar. Sci. Appl., **13**(2), pp. 158–166.
[14] Ye, H., Shen, Z., and Wan, D.C. 2012, "Numerical Prediction of Added Resistance and Vertical Ship Motions in Regular Head Waves," J. Mar. Sci. Appl., **11**(4), pp. 410–416.
[15] Shen, Z., and Wan, D.C. 2013, "RANS Computations of Added Resistance and Motions of a Ship in Head Waves," Int. J. Offshore Polar Eng., **23**(04), pp. 264–271.
[16] Shen, Z., Ye, H., and Wan, D.C. 2014, "URANS Simulations of Ship Motion Responses in Long-Crest Irregular Waves," J. Hydrodyn. Ser B, **26**(3), pp. 436–446.
[17] Wang, J., Zhao, W., and Wan, D.C. 2016, "Self-Propulsion Simulation of ONR Tumblehome Using Dynamic Overset Grid Method," *Proceedings of 7th International Conference on Computational Methods*, Berkeley, CA, USA.
[18] Wang, J., Liu, X., Wan, D.C. and Chen, G. 2016, "Numerical Prediction of KCS Self-Propulsion in Shallow Water," *Proceedings of 26th International Ocean and Polar Engineering Conference*, pp. 757–763.
[19] Wang, J., Zou, L., and Wan, D.C. 2017, "CFD Simulations of Free Running Ship under Course Keeping Control," Ocean Eng., **141**, pp. 450–464.
[20] Berberović, E., van Hinsberg, N., Jakirlić, S., Roisman, I., and Tropea, C. 2009, "Drop Impact onto a Liquid Layer of Finite Thickness: Dynamics of the Cavity Evolution," Phys. Rev. E, **79**(3), 36306.
[21] Menter, F. R., Kuntz, M., and Langtry, R. 2003, "Ten Years of Industrial Experience with the SST Turbulence Model," Turbul. Heat Mass Transf., **4**(1), pp. 625–632.
[22] Issa, R. I. 1986, "Solution of the Implicitly Discretised Fluid Flow Equations by Operator-Splitting," J. Comput. Phys., **62**(1), pp. 40–65.
[23] Elshiekh, H. 2014, "Maneuvering Characteristics in Calm Water and Regular Waves for ONR Tumblehome," The University of IOWA.
[24] Sanada, Y., Elshiekh, H., Toda, Y., and Stern, F. 2014, "Effects of Waves on Course Keeping and Maneuvering for Surface Combatant ONR Tumblehome," *Proceedings of 30th Symposium on Naval Hydrodynamics*, Hobart, Australia.